Circulation

ORIGINAL RESEARCH ARTICLE

Ankyrin-B Q1283H Variant Linked to Arrhythmias Via Loss of Local Protein Phosphatase 2A Activity Causes Ryanodine Receptor Hyperphosphorylation

BACKGROUND: Human loss-of-function variants of *ANK2* (ankyrin-B) are linked to arrhythmias and sudden cardiac death. However, their in vivo effects and specific arrhythmogenic pathways have not been fully elucidated.

METHODS: We identified new *ANK2* variants in 25 unrelated Han Chinese probands with ventricular tachycardia by whole-exome sequencing. The potential pathogenic variants were validated by Sanger sequencing. We performed functional and mechanistic experiments in ankyrin-B knockin (KI) mouse models and in single myocytes isolated from KI hearts.

RESULTS: We detected a rare, heterozygous *ANK2* variant (p.Q1283H) in a proband with recurrent ventricular tachycardia. This variant was localized to the ZU5[C] region of *ANK2*, where no variants have been previously reported. KI mice harboring the p.Q1283H variant exhibited an increased predisposition to ventricular arrhythmias after catecholaminergic stress in the absence of cardiac structural abnormalities. Functional studies illustrated an increased frequency of delayed afterdepolarizations and Ca^{2+} waves and sparks accompanied by decreased sarcoplasmic reticulum Ca^{2+} content in KI cardiomyocytes on isoproterenol stimulation. The immunoblotting results showed increased levels of phosphorylated ryanodine receptor Ser2814 in the KI hearts, which was further amplified on isoproterenol stimulation. Coimmunoprecipitation experiments demonstrated dissociation of protein phosphatase 2A from ryanodine receptor in the KI hearts, which was accompanied by a decreased binding of ankyrin-B to protein phosphatase 2A regulatory subunit B56α. Finally, the administration of metoprolol or flecainide decreased the incidence of stress-induced ventricular arrhythmias in the KI mice.

CONCLUSIONS: *ANK2* p.Q1283H is a disease-associated variant that confers susceptibility to stress-induced arrhythmias, which may be prevented by the administration of metoprolol or flecainide. This variant is associated with the loss of protein phosphatase 2A activity, increased phosphorylation of ryanodine receptor, exaggerated delayed afterdepolarization-mediated trigger activity, and arrhythmogenesis.

Wengen Zhu, MD*
Cen Wang, MD*
Jinzhu Hu, MD, PhD*
Rong Wan, PhD
Jianhua Yu, MD
Jinyan Xie, MS
Jianyong Ma, MD, PhD
Linjuan Guo, MD
Jin Ge, MD
Yumin Qiu, MD
Leifeng Chen, MD
Hualong Liu, MD
Xia Yan, MS
Xiuxia Liu, PhD
Jin Ye, MS
Wenfeng He, MD, PhD
Yang Shen, MD, PhD
Chao Wang, PhD
Peter J. Mohler, PhD
Kui Hong, MD, PhD

https://www.ahajournals.org/journal/circ

Clinical Perspective

What Is New?

- We identified the first *ANK2* variant (p.Q1283H) localized to the ZU5^C region in a patient with ventricular tachycardia.
- Knockin mice with the p.Q1283H variant showed an increased susceptibility to arrhythmias associated with abnormal Ca^{2+} dynamics.
- The loss of protein phosphatase 2A activity from ryanodine receptor is likely associated with reduced ankyrin-B/B56α binding, which is the potential mechanism of ryanodine receptor hyperphosphorylation.
- Metoprolol and flecainide are potential therapies for *ANK2* p.Q1283H-associated arrhythmias.

What Are the Clinical Implications?

- Our study indicates that the dysfunction of the ZU5^C region might be responsible for arrhythmias.
- Our findings on *ANK2* variants interfering with the protein phosphatase 2A-related Ca^{2+} signaling pathway would help in the development of a possible antiarrhythmic medication.

Ankyrin-B (AnkB, encoded by *ANK2*) refers to the ankyrin member responsible for the targeting of integral membrane proteins to specialized cellular compartments or organelles.[1–4] Canonical AnkB consists of a highly conserved N-terminal membrane-binding domain with 24 *ANK* repeats, a spectrin-binding domain (SBD) with a ZU5^N-ZU5^C-UPA tandem, and a regulatory domain (RD) composed of a death domain and a variable C-terminal domain. In the SBD, ZU5^N interacts with spectrin, thereby linking membrane-binding domain-associated binding partners to the spectrin/actin-based cytoskeleton, whereas the function of ZU5^C and UPA are still poorly defined.[5] Human loss-of-function *ANK2* variants as well as variants that decrease AnkB expression have been linked to a wide spectrum of arrhythmias termed ankyrin-B syndrome,[1,2] such as sinus node dysfunction, atrial fibrillation, long QT syndrome, ventricular tachycardia (VT), idiopathic ventricular fibrillation, catecholaminergic polymorphic VT (CPVT), and sudden cardiac death.[4] In vitro studies have shown that cellular afterdepolarizations and extrasystoles because of abnormal Ca^{2+} cycling are the underlying causes of arrhythmogenesis.[1,3] However, no comprehensive studies have explored the in vivo effects and precise arrhythmogenic mechanisms of *ANK2* variants.

AnkB-deficient mice (AnkB$^{+/-}$) display an arrhythmia phenotype similar to that in human *ANK2* variant carriers, which is partly mediated by ryanodine receptor (RyR2)-associated sarcoplasmic reticulum (SR) Ca^{2+} release.[3,6] However, the specific molecular events leading to RyR2 hyperactivity have not been extensively studied. Protein phosphatase type 2A (PP2A), which has catalytic, scaffolding, and regulatory subunits, can regulate the dephosphorylation of RyR2.[7] Of the 13 PP2A regulatory subunits, B56α appears to control the phosphorylation state of RyR2.[8,9] It is important to note that AnkB is essential for targeting B56α,[10] which tethers PP2A to the RyR2 complex.[9] Herein, we hypothesize that *ANK2* variants may promote the development of arrhythmias through the RyR2-mediated remodeling of Ca^{2+} signaling by interfering with normal PP2A activity.

We performed genetic screening and identified a rare, heterozygous *ANK2* variant (p.Q1283H) localized to ZU5^C in a proband with VT. We generated knockin (KI) mice carrying the p.Q1283H variant, which exhibited an increased predisposition to arrhythmias during epinephrine challenge. The phenotype could be prevented by the administration of metoprolol or flecainide. Cellular electrophysiology and Ca^{2+}-imaging experiments in the KI cardiomyocytes demonstrated an increased frequency of delayed afterdepolarizations (DADs) and arrhythmogenic SR Ca^{2+} release under isoproterenol (ISO) stimulation. Immunoblots revealed that phosphorylation of RyR2 Ser2814 was significantly increased in the KI hearts and was further enhanced by ISO stimulation. Mechanistically, the combination of enhanced adrenergic activity and the loss of local PP2A activity from RyR2, which was likely associated with reduced AnkB/B56α binding, is a potential cause of RyR2 hyperphosphorylation.

METHODS

The data and analytical methods have been made available to other researchers for the purposes of reproducing the results or replicating the procedure. Please refer to the expanded Materials and Methods in the online-only Data Supplement for details.

Human Studies

Human studies were performed in accordance with the Code of Ethics of the World Medical Association (Declaration of Helsinki) and approved by the Ethics Committee of the Second Affiliated Hospital to Nanchang University. Informed consent was obtained from all subjects.

Animal Studies

Animal studies were performed in accordance with the Guide for the Care and Use of Laboratory Animals published by the US National Institutes of Health (Publication No. 85-23, revised 1996) and approved by the Animal Ethics Committee of Nanchang University.

Statistical Analysis

Continuous data are presented as the mean±SEM. For data with a Gaussian distribution, unpaired Student *t* tests (equal variance) or unpaired Student *t* test with Welch's correction (unequal variance) were used for comparisons between

2 independent groups; 1-way ANOVA with post hoc Tukey tests was used for multiple comparisons. For data with a non-Gaussian distribution, we performed a nonparametric statistical analysis using the Mann–Whitney U test for comparisons between 2 groups or the Kruskal–Wallis test for multiple comparisons. Categorical data are expressed as percentages and compared between groups using the Fisher exact test. All analyses were performed using the GraphPad Prism software. Statistical significance was defined as $P<0.05$.

RESULTS

Identification of a Rare Human *ANK2* Variant Associated With VT

We performed whole-exome sequencing in 25 unrelated Han Chinese probands with VT and identified an *ANK2* variant in 1 female proband 53 years of age. This case had a history of recurrent palpitations and syncope
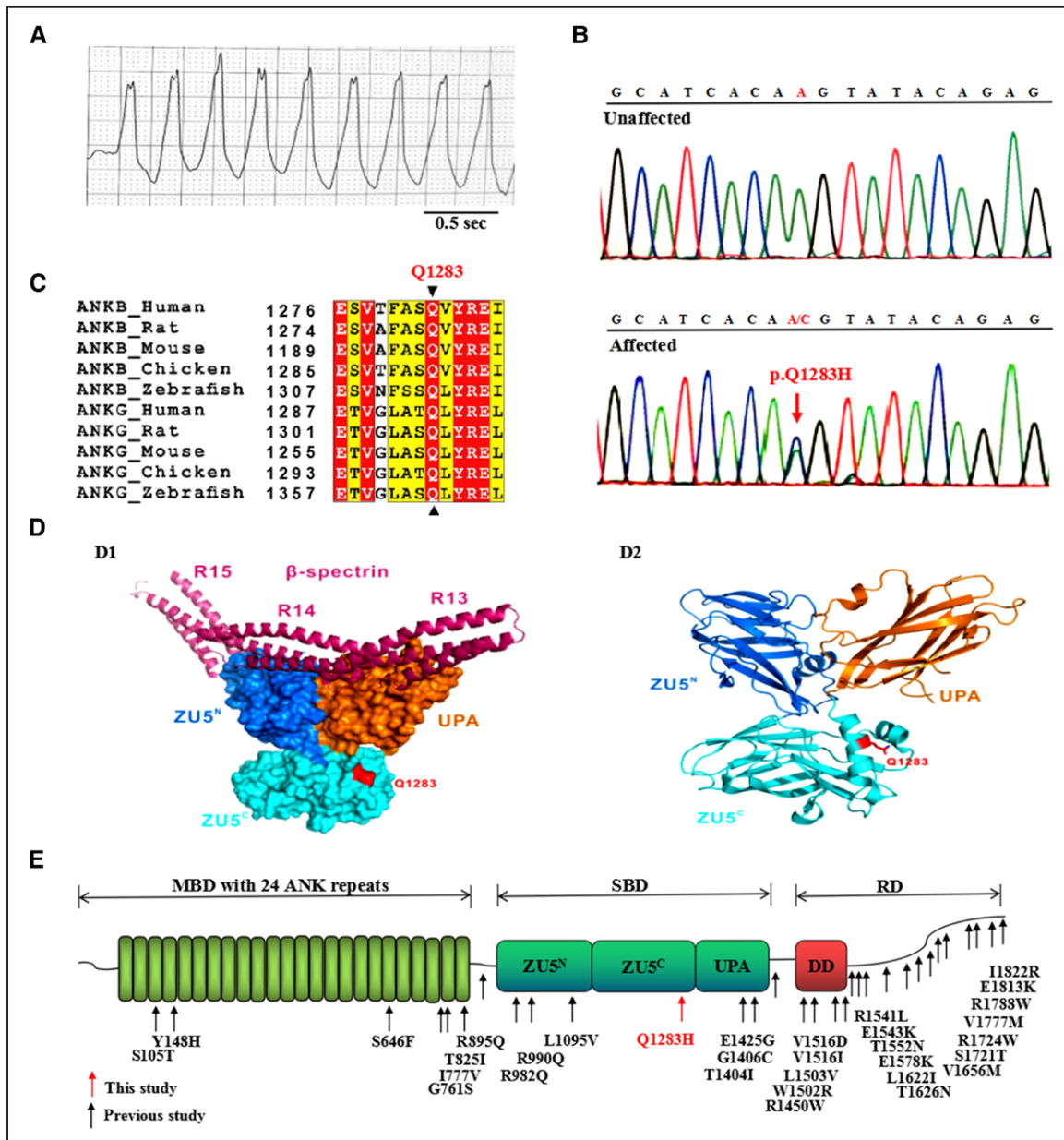

Figure 1. Detection of the *ANK2* p.Q1283H variant in a proband with VT.
A, ECG of the proband showing VT with a normal QTc interval of 430 ms. **B**, Electropherogram showing the WT *ANK2* sequence (**upper**) and the *ANK2* p.Q1283H variant (**lower**, red arrow). This variant represents a heterozygous A-to-C nucleotide substitution (c.A3849C) in exon 33, resulting in a glutamine-to-histidine substitution at position 1283 (p.Q1283H). The c.A3849C and p.Q1283H variants described in this study are equivalent to the c.A3948C and p.Q1316H variants based on NM_020977.4 and NP_066187.2, respectively. **C**, Protein sequence alignment revealing that the p.Q1283 residue of *ANK2* is absolutely conserved across multiple species and isoforms. In this alignment, residues that are absolutely conserved and highly conserved are highlighted in red and yellow, respectively. **D**, Structural model showing that the p.Q1283 residue was localized to the ZU5C domain outside of the spectrin-binding surface (D1). The ribbon structure of the crystal structure of AnkB ZZUD showing the location of the Q1283 residue (D2). The p.Q1283 residue is shown in red. **E**, Mapping of the AnkB domain with *ANK2* variants identified in previous studies (black arrows) and this study (red arrow). Canonical AnkB consists of distinct structural domains: an MBD with 24 ankyrin repeats, an SBD containing 2 ZU5 domains (ZU5N and ZU5C), a UPA domain, and an RD composed of a DD and a CTD. AnkB indicates ankyrin-B; CTD, C-terminal domain; DD, death domain; MBD, membrane-binding domain; QTc, corrected QT; RD, regulatory domain; SBD, spectrin-binding domain; VT, ventricular tachycardia; WT, wild type; and ZZUD, ZU5N-ZU5C-UPA-DD domains.

because of VT (Figure 1A). Her resting ECG showed a normal sinus rhythm, atrioventricular conduction, and QT duration. VT episodes were abated on treatment with a β-blocker (metoprolol). One month after termination of the drug, she reexperienced multiple syncopal episodes because of repeated VT. She subsequently underwent radiofrequency catheter ablation targeting the VT. The patient had no history of other diseases, familial cardiac events, or sudden cardiac death. Echocardiography examination did not detect any structural heart diseases.

Analysis of exome-sequencing data led to identification of 3 heterozygous variants, namely, p.T493I in *CAMK2D*, p.V2189I in *AKAP9*, and p.Q1283H in *ANK2* (Table I and Figure I in the online-only Data Supplement). The *CAMK2D* p.T493I and *AKAP9* p.V2189I variants showed a low pathogenicity potential based on *in silico* prediction algorithms (Table II in the online-only Data Supplement). The *ANK2* p.Q1283H (rs755373114) variant showed a high pathogenicity index and was further validated by Sanger sequencing (Figure 1B). This variant showed a rare minor allele
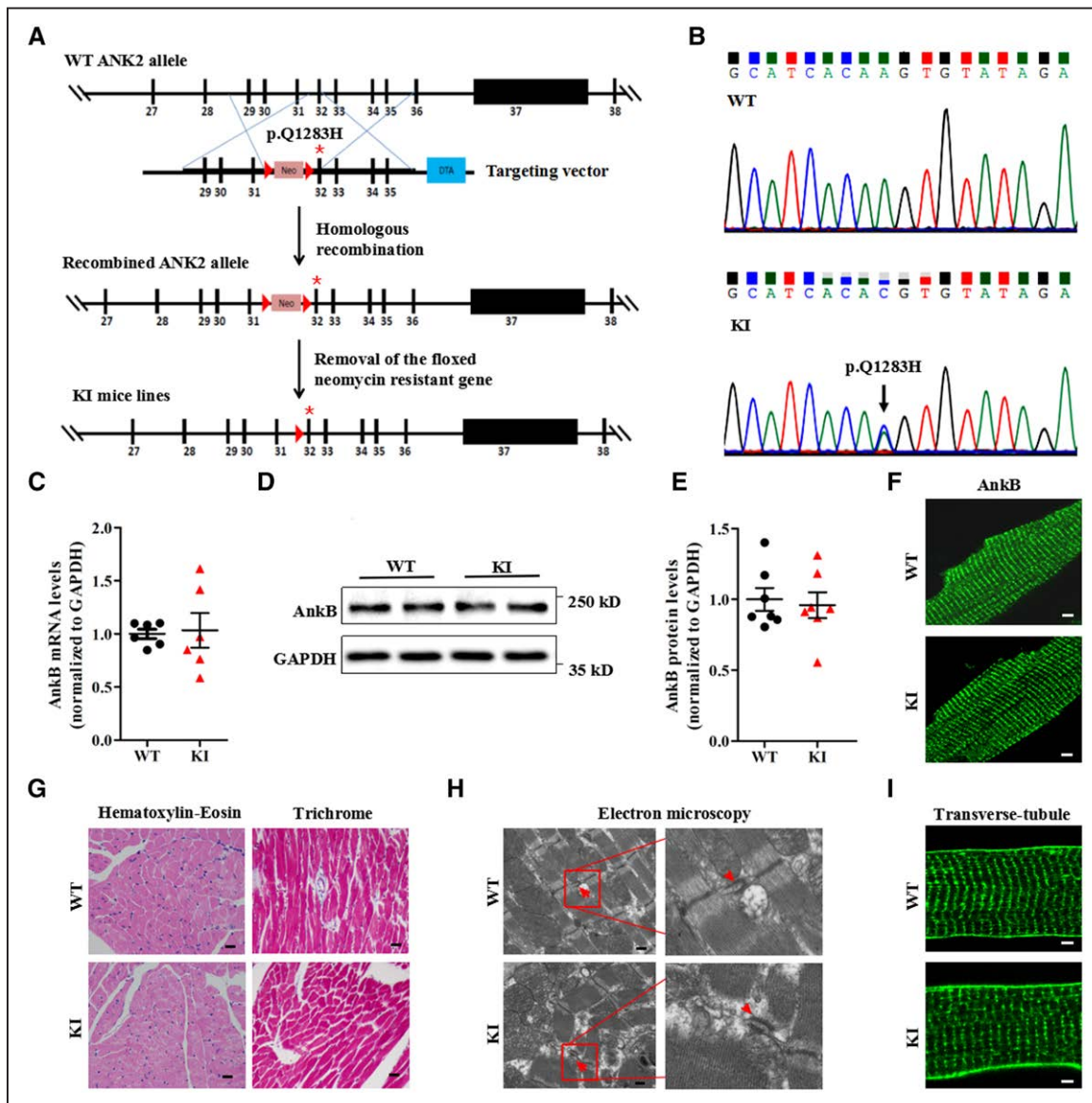

Figure 2. Generation and evaluation of KI mouse models carrying the *ANK2* p.Q1283H variant under basal conditions.
A, Schematic diagram illustrating the targeting vector and step-wise generation of KI mouse models. **B**, DNA sequencing confirming the successful generation of KI mice carrying the p.Q1283H variant (**lower**, black arrow). **C**, Quantitative real-time PCR analysis of AnkB mRNA in sections of the ventricles of WT and KI littermates (n=6 hearts/genotype, *P*=0.85). **D** and **E**, Representative immunoblots (**D**) and quantitative assessment (**E**) of the protein expression level of AnkB in sections of the ventricles of WT and KI littermates (n=7 hearts/genotype, *P*=0.54). **F**, Representative immunostaining showing that cardiomyocytes from WT and KI mice display a normal subcellular distribution of AnkB. **G**, Representative images of hematoxylin-eosin staining (**left**; magnification ×400) and Masson's trichrome staining (**right**; magnification ×400) of left ventricles from WT and KI mice. **H**, Representative electron micrographs of left ventricles from WT and KI mice (red arrowheads indicate the t-tubule lumen marked by the sarcoplasmic reticulum and t-tubule membranes of the triads). **I**, Representative immunostaining showing that cardiomyocytes from WT and KI mice display a normal t-tubule organization (stained with Di-8-ANEPPs). The data shown in **F** through **I** are representative of ≥3 hearts/genotype. AnkB indicates ankyrin-B; GAPDH, glyceraldehyde-phosphate dehydrogenase; KI, knockin; PCR, polymerase chain reaction; and WT, wild type.

frequency of 0.0008091 (East Asian) in the Exome Aggregation Consortium database. It was absent in 3200 ethnically matched controls and in the 1000 Genomes and ESP6500 databases. The Q1283 residue of *ANK2* is absolutely conserved across species and isoforms (Figure 1C). The crystal structure of AnkB-SBD revealed that the p.Q1283H variant was localized to the surface of the ZU5^C domain (Figure 1D), where no variants have previously been linked with heart diseases (Figure 1E). Family members of the proband with the p.Q1283H variant declined genetic studies.

To test the impact of the p.Q1283H variant on the AnkB polypeptide, we performed a biochemical analysis of purified AnkB-SBD harboring the p.Q1283H variant in parallel with the wild type (WT) and identified similar expression between them (Figure IIA in the online-only Data Supplement). Analytic gel filtration assays using the WT and p.Q1283H mutant proteins with spectrin revealed an identical profile (Figure IIB in the online-only Data Supplement). Isothermal titration calorimetry experiments further confirmed that the dissociation constants between the WT and mutant AnkB proteins with spectrin were similar (Figure IIC in the online-only Data Supplement). Thus, we identified a rare *ANK2* variant localized to the ZU5^C region in a patient with VT, which did not affect the expression or spectrin-binding properties of AnkB.

KI Mice With the p.Q1283H Variant Exhibit Cardiac Arrhythmias in Response to Catecholamines

To characterize in vivo effects of the p.Q1283H variant on cardiac function, we engineered a KI mouse model harboring this variant through homologous recombination (Figure 2A and 2B and Table III in the online-only Data Supplement). In agreement with our biochemical data, the transcriptional and posttranslational expression levels, as well as the localization of AnkB, were indistinguishable between the WT and KI mice (Figure 2C through 2F). Compared with age- and sex-matched WT littermates, the KI mice displayed no alterations in cardiac structure as assessed by echocardiography (Table IV in the online-only Data Supplement) and histopathologic analysis (Figure 2G), or in tissue ultrastructural organization, as assessed by electron microscopy (Figure 2H). We also observed no differences in myocyte ultrastructure, including the t-tubule/SR complex (Figure 2H and 2I), the intercalated disc protein (N-cadherin), and the microfilament and microtubule networks (Figure IIIA in the online-only Data Supplement).

Telemetry monitoring of the cardiac rhythm in conscious animals revealed no differences in the electrocardiographic parameters between the 2 genotypes under sedentary conditions (Figure 3A and 3B and Table V in the online-only Data Supplement). Because both humans with *ANK2* variants and AnkB$^{+/-}$ mice develop

exercise- and catecholamine-induced ventricular arrhythmias and sudden cardiac death,[1,3,11] the KI mice were subjected to a catecholamine stress protocol (an intraperitoneal injection of 2 mg/kg epinephrine). Over a 60-minute continuous recording, KI mice were more susceptible to developing a sinus pause and multiple ventricular arrhythmic patterns, including premature ventricular contractions, bigeminy/trigeminy, and nonsustained or sustained VT episodes (Figure 3C through 3G). Specifically, 7 of the 10 KI mice had an increased incidence of ventricular arrhythmias, whereas only 1 of the 10 WT mice showed an arrhythmia phenotype (70% in KI versus 10% in WT; $P<0.05$) (Figure 3H). No WT mice presented a VT phenotype, but 50% of the KI mice did present a VT phenotype (50% in KI versus 0% in WT; $P<0.05$). None of the VT rhythms deteriorated to ventricular fibrillation or death during the epinephrine challenge. In addition, compared with controls, the KI mice showed a remarkable increase in the arrhythmia score ($P<0.01$) (Figure 3I).[12]

KI Cardiomyocytes Display Delayed Afterdepolarizations and Spontaneous Ca^{2+} Release Under β-Adrenergic Stimulation

To determine the effect of the p.Q1283H variant on myocyte electrophysiological properties, we recorded the action potentials (AP) of the WT and KI cardiomyocytes in the absence or presence of 1 μM ISO. After 10 seconds of pacing to reach steady-state Ca^{2+} transient amplitude, the field stimulation was stopped and afterdepolarizations were recorded. In the absence of ISO, spontaneous afterdepolarizations were nearly absent in both groups. In the presence of ISO plus 2-Hz pacing, 14% (3/21) of the WT cardiomyocytes showed spontaneous DADs, whereas this incidence was increased to 63% (19/30) in the KI cardiomyocytes ($P<0.01$) (Figure 4A and 4B). Moreover, no WT cardiomyocytes showed trigger activity, but 40% (12/30) of the KI cardiomyocytes did show trigger activity ($P<0.01$) (Figure 4C). Under this condition, we observed no differences in the AP duration, AP amplitude, resting membrane potential, or rate of rise of the AP upstroke between the 2 groups (Table VI in the online-only Data Supplement).

Diastolic spontaneous Ca^{2+} release from the SR is a potential electrophysiological basis for the formation of DAD-mediated trigger activity.[13] To evaluate the status of SR Ca^{2+} release, we examined the occurrence of spontaneous Ca^{2+} transients (SCaTs; ie, Ca^{2+} waves) in fluo-4-loaded cardiomyocytes. During pausing after a period of pacing, SCaTs were rarely observed in the 2 groups in the absence of ISO. However, in the presence of ISO plus 2-Hz pacing, 61% (22/36) of the KI cardiomyocytes developed SCaTs compared with 23% (5/22) of the WT cardiomyocytes ($P<0.01$) (Figure 4D
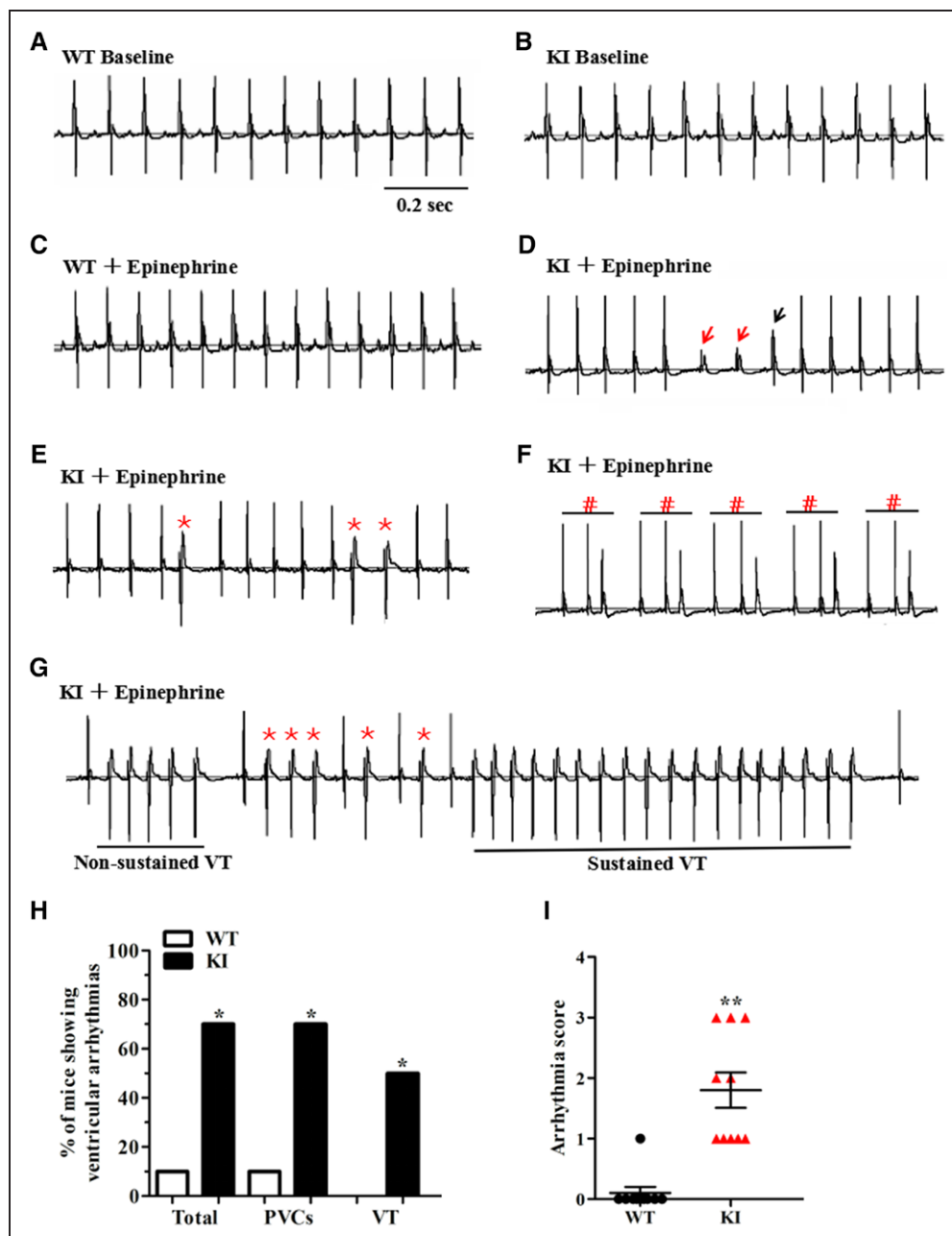
Figure 3. KI mice develop cardiac arrhythmias in response to stress stimulation.
A and **B**, Representative lead-II ECG traces of conscious WT and KI mice at baseline, respectively. **C**, Representative lead-II ECG traces of conscious WT mice after an intraperitoneal injection of 2 mg/kg epinephrine. **D** through **G**, Representative lead-II ECG traces of conscious KI mice after an intraperitoneal injection of 2 mg/kg epinephrine. KI mice display a sinus pause (**D**, the escape rhythm is denoted by red arrows; the ventricular fusion beat is denoted by black arrow) and ventricular arrhythmias, including PVCs (**E**, *), trigeminy (**F**, #), and VT (**G**, both nonsustained and sustained episodes). **H**, Cumulative incidence of ventricular arrhythmias of WT and KI mice under stress conditions (*$P<0.05$; n=10 for WT and KI mice, respectively). **I**, Cumulative data of the arrhythmia scores of WT and KI mice under stress conditions (**$P<0.01$; n=10 for WT and KI mice). KI indicates knockin; PVCs, premature ventricular contractions; VT, ventricular tachycardia; and WT, wild type.

and 4E). Moreover, only 5% (1/22) of the WT cells developed triggered events; however, this incidence was increased to 39% (14/36) in the KI cells ($P<0.01$) (Figure 4F). To test whether spontaneous SR Ca^{2+} release potentially underlies the chaotic electric behavior, the KI cardiomyocytes were pretreated with ryanodine, an agent with a high affinity for RyR2. As shown in Figure 4A through 4F, 100 nmol/L ryanodine significantly inhibited the Ca^{2+} waves and, subsequently, the DADs

and trigger activity in the KI cardiomyocytes under ISO stimulation.

KI Cardiomyocytes Display an Enhanced Ca^{2+} Spark Frequency and a Reduced SR Ca^{2+} Content

Because spontaneous SR Ca^{2+} release primarily manifests as abnormal RyR2 openings,[14] we visualized Ca^{2+}
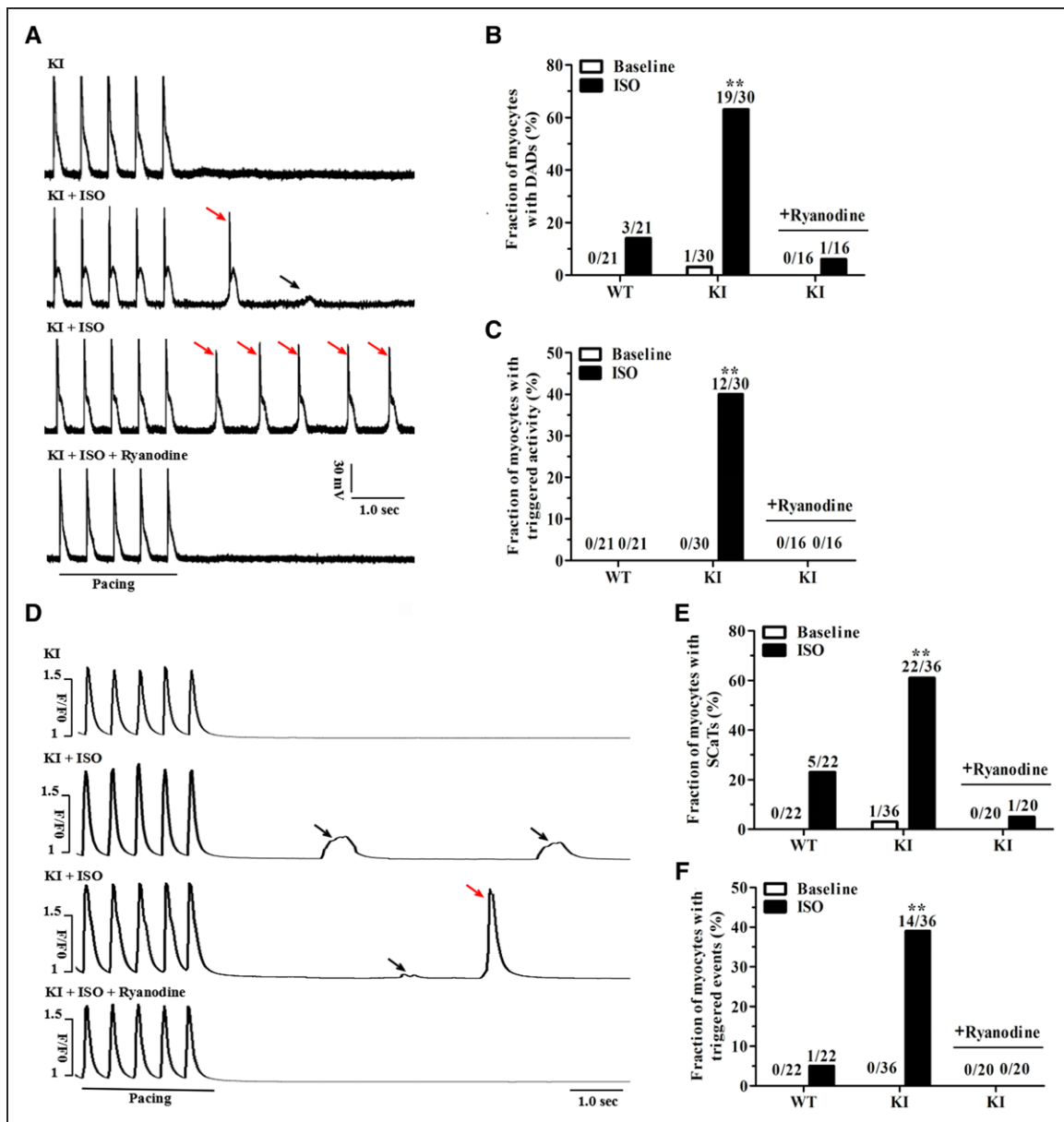
Figure 4. KI cardiomyocytes display stress-induced delayed afterdepolarizations and spontaneous Ca²⁺ release.
A, Representative traces of action potentials in KI cardiomyocytes±1 µM ISO or 100 nmol/L ryanodine. Small DADs (black arrow) and triggered activity (red arrows) were recorded after a stimulation pause after a 2-Hz field stimulation. **B** and **C**, Cumulative incidence of DADs (**B**) and triggered activity (**C**) in WT and KI cardiomyocytes (n=16–30 cells per group from 5 hearts/genotype; **P<0.01 versus WT+ISO or versus KI+ISO+ryanodine). **D**, Representative traces of the occurrence of SCaTs (black arrows) and triggered beats (red arrow) after a stimulation pause after 2-Hz field stimulation in KI cardiomyocytes±1 µM ISO or 100 nmol/L ryanodine. **E** and **F**, Cumulative incidence of SCaTs (**E**) and triggered beats (**F**) in WT and KI cardiomyocytes (n=20–36 cells per group from 5 hearts/genotype; **P<0.01 versus WT+ISO or versus KI+ISO+ryanodine). DADs indicates delayed afterdepolarizations; ISO, isoproterenol; KI, knockin; SCaTs, spontaneous Ca²⁺ transients; SR, sarcoplasmic reticulum; and WT, wild type.

sparks in quiescent fluo-4-loaded cardiomyocytes. As presented in Figure 5A and 5B, the frequency of Ca²⁺ sparks was significantly increased in the KI cardiomyocytes without ISO stimulation (2.05±0.12 in KI versus 1.27±0.10 sparks/100 µm⁻¹ s⁻¹ in WT; $P<0.01$). In the presence of ISO, the Ca²⁺ spark frequency was further enhanced (3.09±0.23 in KI versus 2.17±0.17 sparks/100 µm⁻¹ s⁻¹ in WT; $P<0.01$). In addition, other Ca²⁺ spark characteristics were unchanged in the KI cardiomyocytes (Table VII in the online-only Data Supplement).

To determine whether aberrant Ca²⁺ sparks affect the cardiac systolic process, we compared the Ca²⁺ handling characteristics between the WT and KI cardiomyocytes. As shown in Figure 5C and 5E, the amplitudes of field-stimulated Ca²⁺ transients, and the average decay-time constants were similar between the 2 groups with or without ISO stimulation. Caffeine-induced Ca²⁺ transients were assessed by the rapid application of 10 mM caffeine after the cessation of pacing. Judging from the amplitude of the caffeine-in-
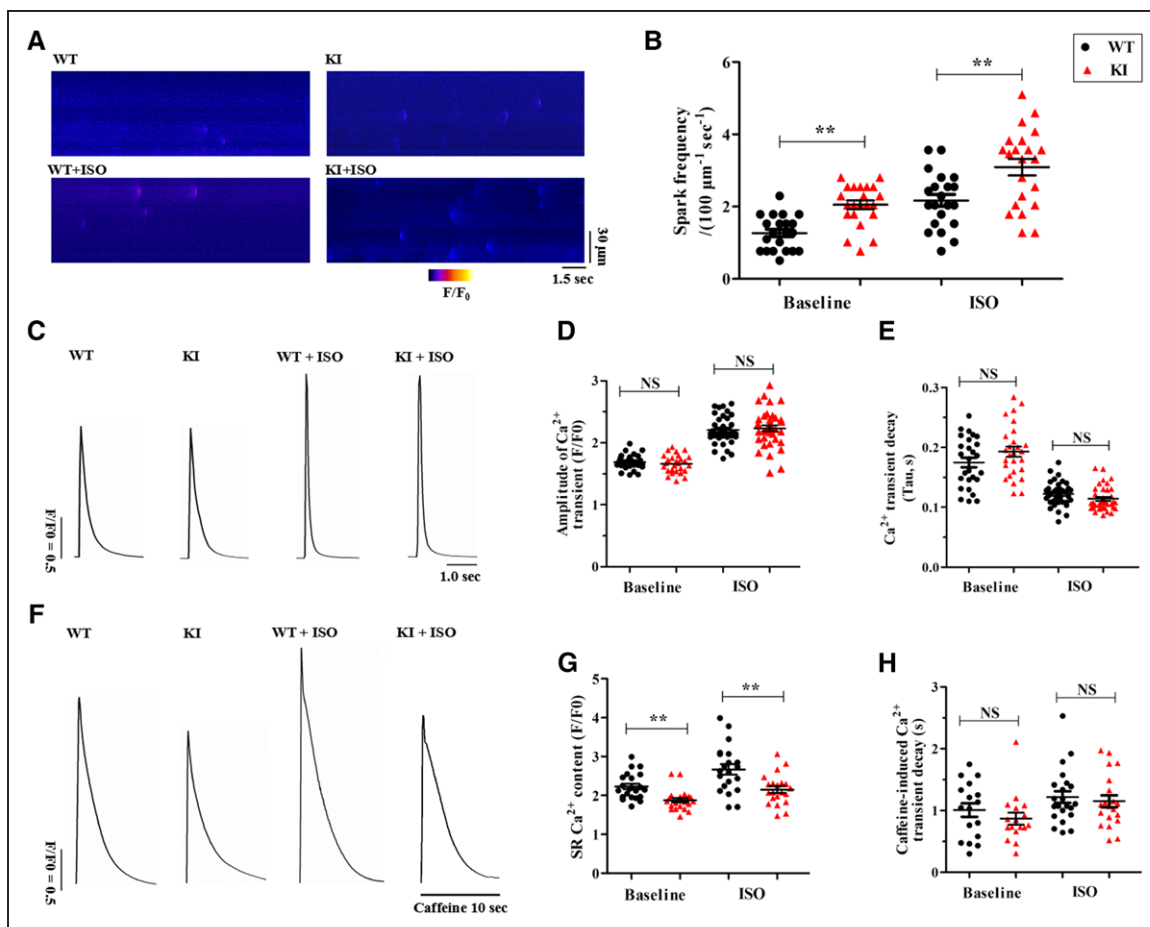
Figure 5. KI cardiomyocytes display an increased Ca²⁺ spark frequency and reduced SR Ca²⁺ content.

A, Representative line-scan images of Ca²⁺ sparks in WT and KI cardiomyocytes±1 μM ISO. **B**, Cumulative data of the Ca²⁺ spark frequency in WT and KI cardio-myocytes (n=21–22 cells per group from 5 hearts/genotype; **P<0.01). **C**, Representative traces of field-stimulated Ca²⁺ transients in WT and KI cardiomyocytes±1 μM ISO. **D** and **E**, Cumulative data of the amplitude of field-stimulated Ca²⁺ transients (**D**, P=NS) and decay-time constants (**E**, P=NS) in WT and KI cardiomyo-cytes±1 μM ISO (n=27–37 cells per group from 5 hearts/genotype). **F**, Representative traces of caffeine-induced Ca²⁺ transients in WT and KI cardiomyocytes±1 μM ISO. **G** and **H**, Cumulative data of the amplitude of caffeine-induced Ca²⁺ transients (ie, SR Ca²⁺ content; **G**, **P<0.01) and decay-time constants (**H**, P=NS) in WT and KI cardiomyocytes ± ISO (n=17–22 cells per group from 5 hearts/genotype). ISO indicates isoproterenol; KI, knockin; NS, not significant; SR, sarcoplasmic reticulum; and WT, wild type.

duced Ca²⁺ transients, compared with their WT coun-terparts, the KI cardiomyocytes showed a significantly decreased SR Ca²⁺ content in both the absence and presence of ISO (Figure 5F and 5G). However, the Ca²⁺ decay-time constant during the caffeine-induced Ca²⁺ transients, which reflects the activity of Na⁺/Ca²⁺ ex-changer type 1,[15] showed no difference between the 2 groups (Figure 5H).

Enhanced Phosphorylation of RyR2 Contributes to Spontaneous Ca²⁺ Release in KI Cardiomyocytes

Despite the changes in electric activity observed in the KI cardiomyocytes, we observed no differences in the protein level of Kv7.1, Nav1.5, or connexin-43 be-tween the experimental groups (Figure IV in the on-line-only Data Supplement). To further investigate the molecular mechanisms of abnormal intracellular Ca²⁺

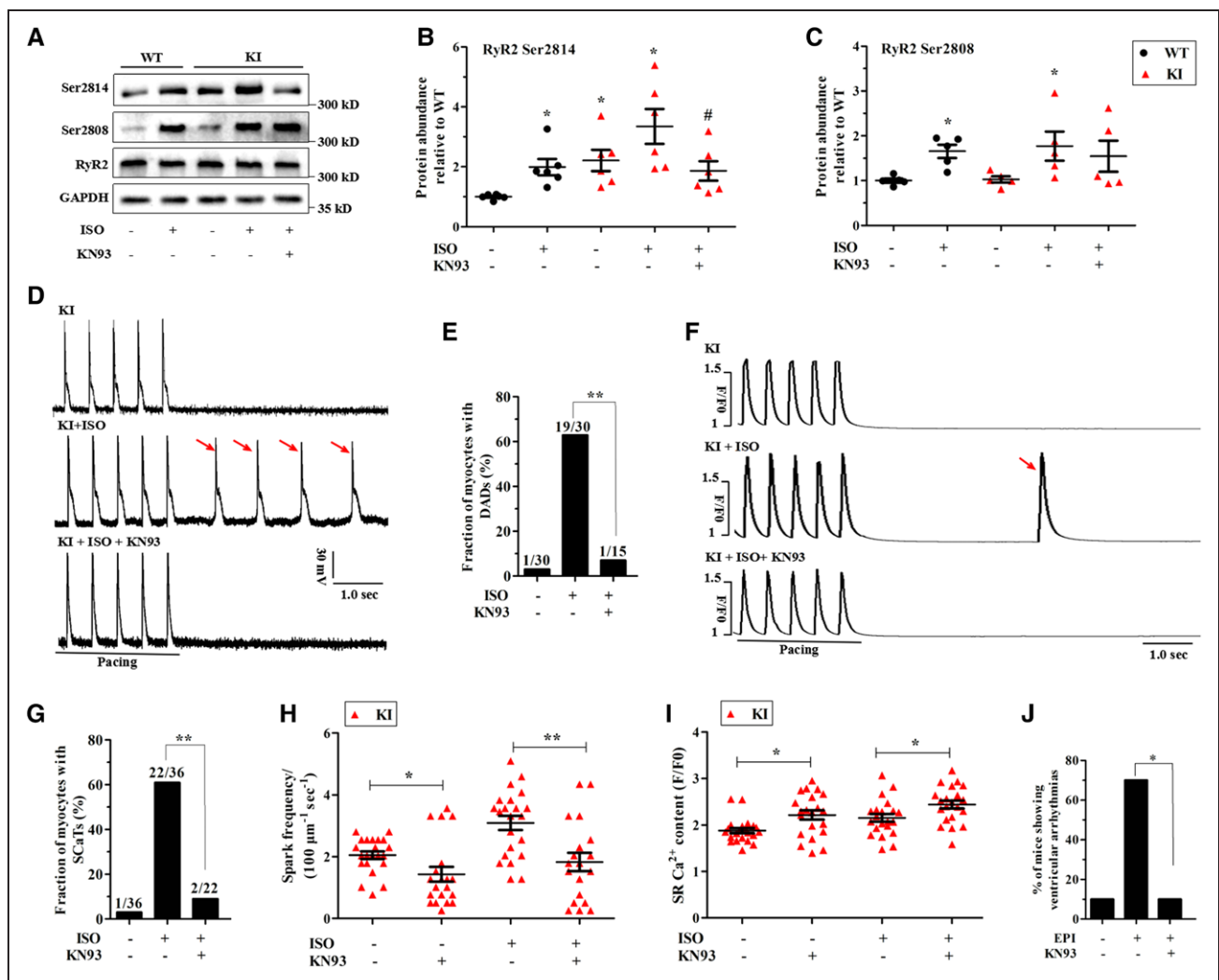cycling, we performed immunoblotting and imaging analyses to determine possible changes in t-tubule/SR membrane-associated Ca²⁺-cycling regulatory pro-teins. However, we did not observe any alterations in the expression or subcellular distribution of sarcolem-mal proteins, including Na⁺/Ca²⁺ exchanger type 1, Na⁺/K⁺ ATPase α1/α2, and the L-type calcium channel (Cav1.2), or in SR membrane proteins, including RyR2, inositol 1,4,5-trisphosphate receptor, SR Ca²⁺ adenos-ine triphosphatase 2, phospholamban (PLN), and calse-questrin 2 (Figures IIIB and V in the online-only Data Supplement).

The posttranslational modification of Ca²⁺-cycling proteins is tightly regulated by adrenergic signaling pathways, which is a potent mechanism for modu-lating functional SR Ca²⁺ release.[16] Therefore, we tested the phosphorylation status of RyR2, Cav1.2, and PLN at both the cAMP-dependent protein ki-nase A and calcium/calmodulin-dependent kinase II

(CaMKII) sites. Consequently, the phosphorylation status of Cav1.2 and PLN showed no changes in the KI hearts (Figure V in the online-only Data Supplement). However, the data presented in Figure 6A through 6C demonstrated that the phosphorylation of RyR2 at the CaMKII site (Ser2814) was significantly increased in the KI myocardium under basal conditions and further enhanced in the presence of ISO, whereas its phosphorylation at the protein kinase A site (Ser2808) was comparable between the experimental groups.

To further test whether an increased level of RyR2 Ser2814 was responsible for the functional changes, a potent CaMKII inhibitor, KN93 (1 µM),[17] was applied to the KI hearts in the absence or presence of ISO.

As expected, KN93 significantly blunted the ISO-induced increase in RyR2 Ser2814 and had no effect on Ser2808 (Figure 6A through 6C). The functional consequences of this effect on RyR2 were that KN93 significantly reversed the DADs and Ca^{2+} waves that were induced by ISO as well as the Ca^{2+} spark frequency and the SR Ca^{2+} content under basal and stress conditions (Figure 6D through 6I). As with KN-93, 1 µM AIP II,[18] a highly selective peptide inhibitor, also alleviated these functional consequences (Figure VI in the online-only Data Supplement). It is important to note that after an intraperitoneal injection of 30 µmol/kg KN93, only 1 of the 10 KI mice suffered from ventricular arrhythmias during epinephrine challenge (P<0.05 versus no drug) (Figure 6J).

Figure 6. CaMKII-dependent phosphorylation of RyR2 and functional effects of CaMKII inhibition in KI hearts.
A through **C**, Representative immunoblots (A) and quantitative assessment of the protein and phosphorylation levels of RyR2 at Ser2814 (**B**; *P<0.05 versus WT at baseline; #P<0.05 versus KI+ISO; n=6 hearts/genotype) and Ser2808 (**C**; *P<0.05 versus WT at baseline; n=5 hearts/genotype) from left ventricle sections in littermates of WT and KI perfused hearts±1 µM ISO or 1 µM KN93. **D** and **E**, Representative traces of the action potentials (**D**) and cumulative incidence of DADs (**E**; **P<0.01) after a stimulation pause after a 2-Hz field stimulation in KI cardiomyocytes±1 µM ISO or 1 µM KN93. **F** and **G**, Representative traces of SCaTs (**F**) and the cumulative incidence of SCaTs (**G**; **P<0.01) after a stimulation pause after a 2-Hz field stimulation in KI cardiomyocytes±1 µM ISO or 1 µM KN93. **H**, Cumulative data of Ca^{2+} spark frequency in KI cardiomyocytes±ISO (*P<0.05; **P<0.01). **I**, Cumulative data of caffeine-induced Ca^{2+} transient amplitude (ie, SR Ca^{2+} content) in KI cardiomyocytes±ISO (*P<0.05). **J**, Cumulative incidence of ventricular arrhythmias in KN93-pretreated KI mice after an intraperitoneal injection of 2 mg/kg epinephrine (*P<0.05; n=10 KI mice for each group). CaMKII indicates calcium/calmodulin-dependent kinase II; DADs, delayed afterdepolarizations; GAPDH, glyceraldehyde-phosphate dehydrogenase; ISO, isoproterenol; KI, knockin; RyR2, ryanodine receptor type 2; SCaTs, spontaneous Ca^{2+} transients; and WT, wild type.

Enhanced Phosphorylation of RyR2 Is Likely Determined by the Loss of Local Phosphatase Activity in KI Cardiomyocytes

The RyR2 complex is bound to kinases and phosphatases that modulate RyR2 in a phosphorylation-dephosphorylation dynamic balance.[16,19] Either an increase in kinase activity or a decrease in phosphatase activity may be responsible for the hyperphosphorylation of RyR2. The immunoblotting analysis did not show any changes in the expression of the protein kinase A catalytic subunit or in CaMKII and its phosphorylation and oxidation (Figure VIIA and VIIB in the online-only Data Supplement). In addition, we did not observe any changes in the phosphoryla-
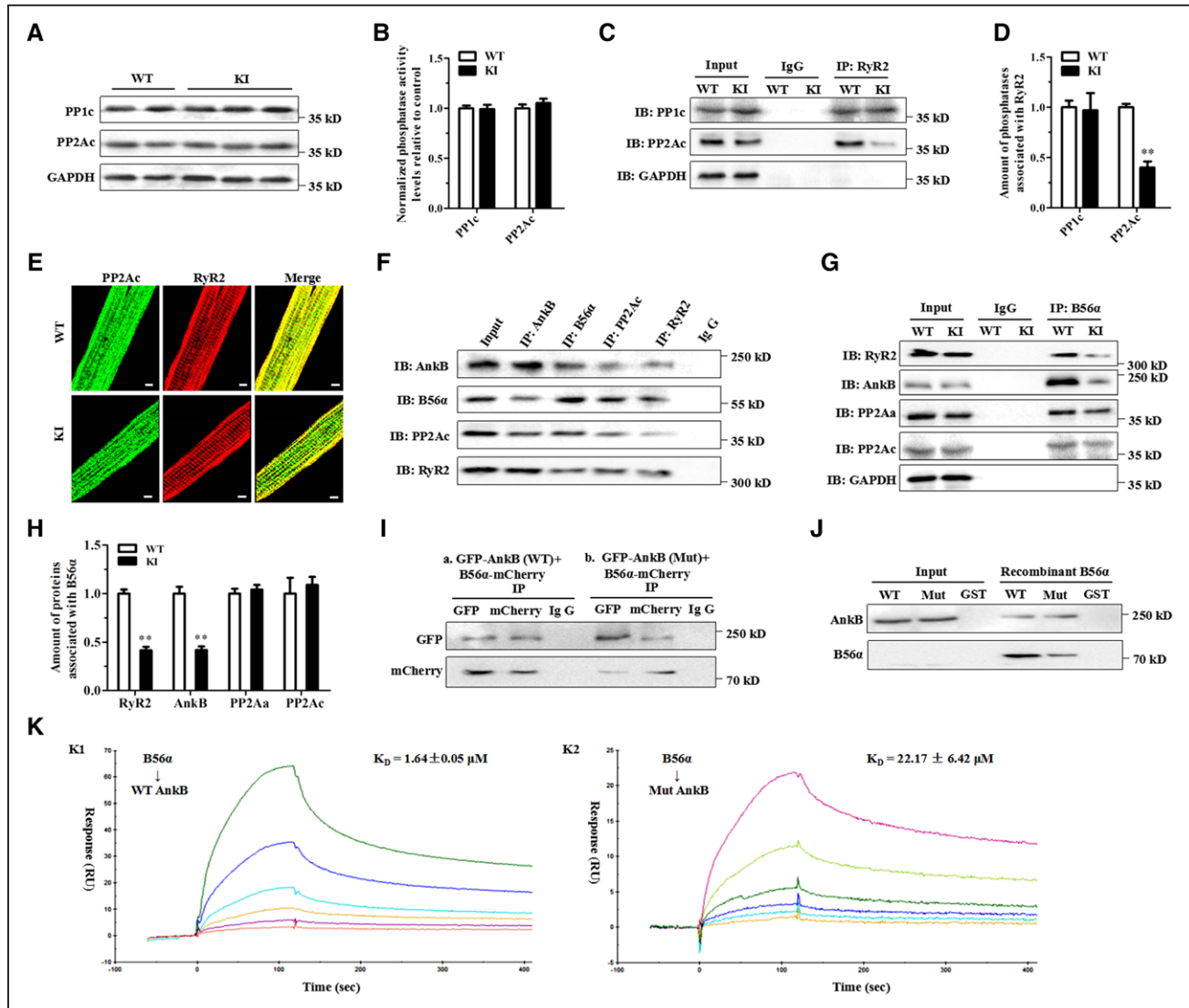

Figure 7. The p.Q1283H variant affects the integration of RyR2 with PP2Ac likely because of decreased AnkB binding of B56α.
A, Representative immunoblots of the expression levels of relevant phosphatases (PP1c and PP2Ac) from left ventricle sections in littermates of WT and KI mice. **B**, Protein phosphatase assays using a fluorescence-based kit for measuring the total PP1 and PP2A activities in heart homogenates from WT and KI mice. **C** and **D**, Representative immunoblots (**C**) and quantitative assessment (**D**) of PP1c and PP2Ac coimmunoprecipitated with RyR2 showing a reduced amount of PP2Ac associated with RyR2 (****P<0.01**), but the interaction of PP1c with RyR2 was not affected in KI hearts. **E**, Representative immunofluorescence assays of WT (**upper**) and KI (**lower**) cardiomyocytes coimmunolabeled with PP2Ac (**left**, green) and RyR2 (**middle**, red) specific antibodies. **F**, Representative coimmunoprecipitation assays showing a macromolecular complex composed of AnkB, B56α, PP2Ac, and RyR2. Total protein homogenates from mouse left ventricles were immunoblotted with either an anti-RyR2 antibody or with antibodies that recognize AnkB, B56α, and PP2Ac, all of which were detected in immunoprecipitates, whereas control preimmune serum (IgG) did not immunoprecipitate the proteins. **G** and **H**, Representative coimmunoprecipitation assays (**G**) and quantitative assessment (**H**) using the anti-B56α antibody as bait showing decreased binding of RyR2 (****P<0.01**) or AnkB (****P<0.01**) with B56α, but the abundance of PP2Aα or PP2Ac binding with B56α was unchanged in KI hearts. **I**, Coimmunoprecipitation from HEK293 cells expressing GFP-tagged mutant AnkB and mCherry-tagged B56α showing a reduced binding of AnkB to B56α. **J**, Representative GST pull-down assays showing that GST-labeled WT AnkB pulled down recombinant B56α, but GST-labeled mutant AnkB showed a decreased binding to B56α. **K**, BIAcore-binding properties of WT (K1: K_D=1.64±0.05 μM) or mutant (K2: K_D=22.17±6.42 μM) AnkB-purified proteins to B56α. AnkB indicates ankyrin-B; HEK, human embryonic kidney; GAPDH, glyceraldehyde-phosphate dehydrogenase; IB, immunoblots; IP, immunoprecipitation; ISO, isoproterenol; KI, knockin; KI, knockin; PP1c, PP1 catalytic subunit; PP2Aα, PP2A scaffolding subunit; PP2Ac, PP2A catalytic subunit; RU, response unit; RyR2, ryanodine receptor type 2; and WT, wild type.

tion status of other protein kinase A (Cav1.2-Ser1928 and PLN-Ser16) or CaMKII (Cav1.2-Ser1512 and PLN-Thr17) targets. Furthermore, coimmunoprecipitation experiments revealed no changes in the abundance of CaMKII that was physically associated with RyR2 in the KI hearts (Figure VIIC in the online-only Data Supplement). These findings reduce the possibility that the enhanced phosphorylation of RyR2 is caused by increased kinase activity.

Protein phosphatase type 1 (PP1) and PP2A are responsible for >90% of dephosphorylation events.[7] However, our immunoblotting analysis found no differences in the expression of the catalytic subunits of PP1 (PP1c) and PP2A (PP2Ac) between the WT and KI hearts (Figure 7A). Phosphatase activity assays showed no differences in the total activity of PP1 and PP2A in samples from both heart homogenates (Figure 7B). However, coimmunoprecipitation assays showed a significantly
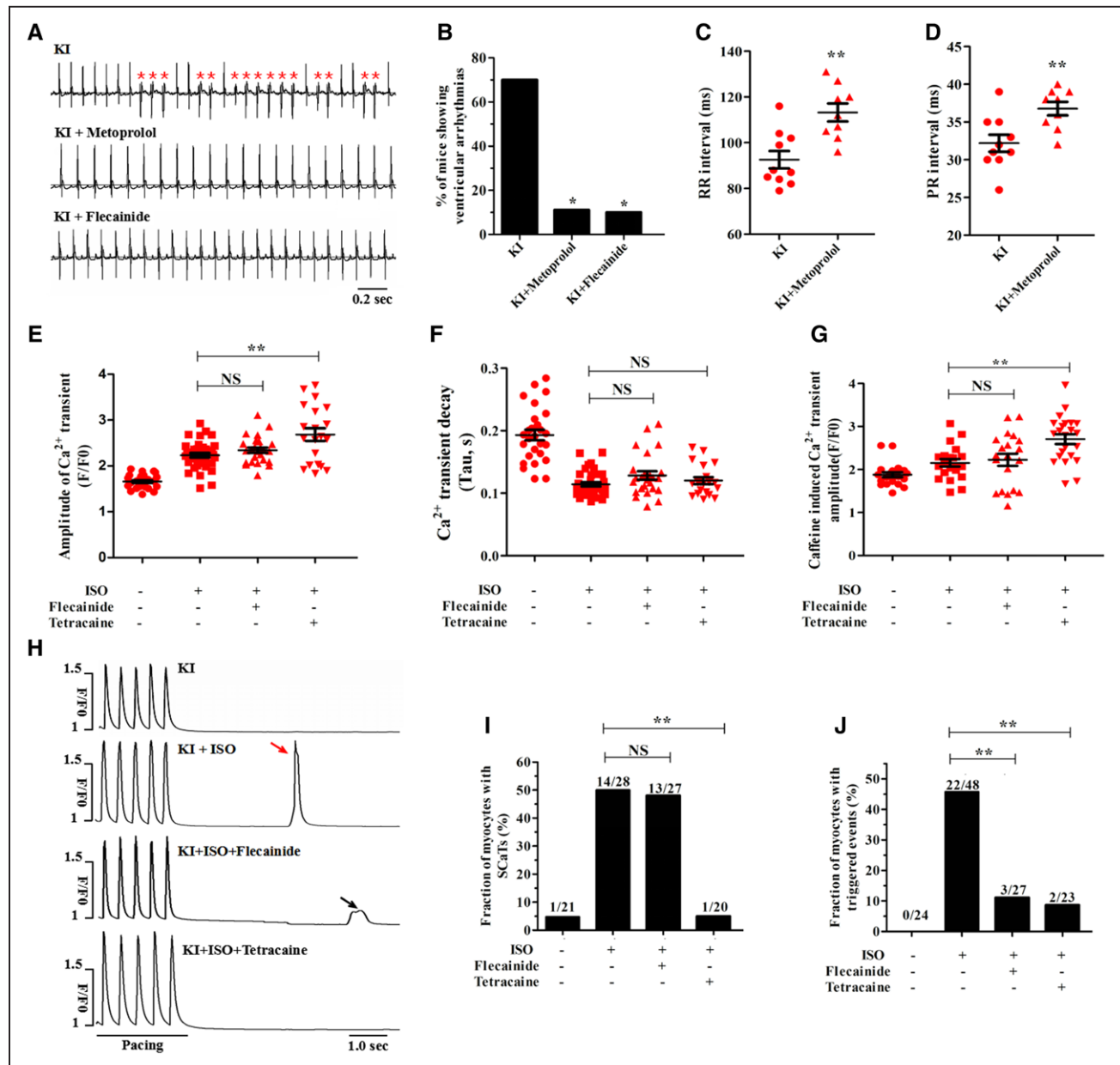

Figure 8. Effect of drug therapy on the stress-induced arrhythmia burden in KI mice.
A, ECG recordings of KI mice pretreated with metoprolol or flecainide after an intraperitoneal injection of 2 mg/kg epinephrine (PVCs were denoted by red asterisks). **B**, Cumulative incidence of ventricular arrhythmias in KI mice after administration of metoprolol (*$P<0.05$ versus no drug) or flecainide (*$P<0.05$ versus no drug). **C** and **D**, Cumulative data of RR (**C**, **$P<0.01$ versus no drug) and PR (**D**, **$P<0.01$ versus no drug) intervals in metoprolol-pretreated KI mice. **E** through **G**, Cumulative data of the field-stimulated Ca²⁺ transient amplitude (**E**, n=20–37 cells per group; P=NS for KI+ISO+flecainide versus KI+ISO; **$P<0.01$ for KI+ISO + tetracaine versus KI+ISO), field-stimulated Ca²⁺ transient decay-time constants (**F**, n=20–37 cells per group; P=NS) and caffeine-induced Ca²⁺ transient amplitude (**G**, n=20–23 cells per group; P=NS for KI+ISO+flecainide versus KI+ISO; **$P<0.01$ for KI+ISO + tetracaine versus KI+ISO) of KI cardiomyocytes. **H** through **J**, Representative images (**H**) and cumulative data showing that tetracaine but not flecainide decreased the incidence of ISO-induced SCaTs (**I**, n=20–28 cells per group; P=NS for KI+ISO+flecainide versus KI+ISO; **$P<0.01$ for KI+ISO+tetracaine versus KI+ISO) and that both tetracaine and flecainide decreased the incidence of ISO-induced triggered beats (**J**, n=23–48 cells per group; **$P<0.01$) in KI cardiomyocytes. ISO indicates isoproterenol; KI, knockin; NS, not significant; PVCs, premature ventricular contractions; SCaTs, spontaneous Ca²⁺ transients.

reduced amount of PP2Ac associated with RyR2, but the interaction of PP1c with RyR2 was not affected in the KI hearts (Figure 7C and 7D). Consistently, confocal images showed decreased colocalization of PP2Ac and RyR2 in the KI cardiomyocytes (Figure 7E). We provide evidence that, at least in part, RyR2 hyperphosphorylation is because of a decrease in the targeting of PP2Ac to RyR2.

Local PP2A activity appears to be controlled by reversible posttranslational modifications of PP2Ac, including tyrosine phosphorylation (Tyr-307) and leucine methylation (Leu-309),[20] or is linked to the PP2A regulatory subunits,[21] including B56α,[10] B56δ,[22,23] and PR130[24] that tether the PP2A holoenzyme to RyR2. However, we found no differences in their expression levels between KI versus WT hearts (Figure VIII in the online-only Data Supplement). Because B56α has been demonstrated to interact with AnkB,[10] we hypothesized that a decrease in PP2A activity localized to RyR2 would reflect the central role of AnkB in targeting B56α. For this purpose, our coimmunoprecipitation experiments on mouse heart homogenates showed that the RyR2 macromolecular complex encompassed B56α, PP2Ac, the PP2A scaffolding subunit (PP2Aα), and AnkB (Figure 7F). Notably, immunoprecipitation studies demonstrated a significantly decreased binding of AnkB or RyR2 with B56α, but the abundance of PP2Aα or PP2Ac binding with B56α was unchanged in the KI hearts (Figure 7G and 7H). Furthermore, coimmunoprecipitation experiments on the lysates of human embryonic kidney 293 cells expressing GFP-tagged mutant AnkB and mCherry-tagged B56α demonstrated a reduced binding of AnkB to B56α (Figure 7I). GST-labeled WT AnkB could pull down the recombinant B56α protein, but GST-labeled mutant AnkB decreased its binding to B56α (Figure 7J). Further surface plasmon resonance experiments revealed that the purified recombinant AnkB could bind to B56α, whereas the mutant AnkB proteins led to a reduced binding affinity with B56α (Figure 7K).

Effect of Drug Therapy on the Stress-Induced Arrhythmia Burden in KI Mice

To evaluate the antiarrhythmic potential of β-blocker therapy during epinephrine challenge, the KI mice were pretreated with 100 mg/kg/d metoprolol for 3 weeks. In contrast to untreated KI mice, only 1 of 9 metoprolol-pretreated animals suffered from stress-induced ventricular arrhythmias ($P<0.05$) (Figure 8A and 8B). The expected changes of prolonged RR and PR intervals typically resulting from metoprolol therapy were observed (Figure 8C and 8D and Table V in the online-only Data Supplement). However, the effect of metoprolol on these parameters was similar between the WT and KI mice (Figure IX in the online-

only Data Supplement). M-mode echocardiogram tracings indicated no alterations in the contractile or structural parameters of the KI mice pretreated with metoprolol (Table IV in the online-only Data Supplement). In the KI cardiomyocytes, ISO stimulation increased the amplitude and decay of field-stimulated Ca^{2+} transients, but metoprolol counteracted these β-adrenergic effects (Figure X in the online-only Data Supplement).

Flecainide (a class I$_C$ antiarrhythmic drug) has been increasingly accepted to be an effective agent for suppressing CPVT in mouse models[25] and clinical patients.[26] The underlying mechanism of action of flecainide is linked, although not exclusively, to the suppression of SR Ca^{2+} release through RyR2.[27] We assessed the therapeutic role of flecainide (15 mg/kg) in KI mice during the epinephrine challenge. As a result, only 1 of 10 KI mice pretreated with flecainide displayed ventricular arrhythmias ($P<0.05$ versus no drug) (Figure 8A and 8B). In the KI cardiomyocytes with ISO stimulation, 50 μM tetracaine (incubation for 3 minutes) increased the Ca^{2+} transient amplitude and SR Ca^{2+} content, but 6 μM flecainide (incubation for 30 minutes) had no effects on these parameters (Figure 8E through 8G). Accordingly, flecainide had no effect on the incidence of SCaTs elicited by ISO, whereas tetracaine reduced this incidence from 50% to 5% (Figure 8H and 8I). In contrast, both tetracaine and flecainide decreased the incidence of triggered events (Figure 8J).

DISCUSSION

In the present study, we identified a rare p.Q1283H variant in the ZU5^C region of *ANK2*, which is associated with VT. The p.Q1283H is a disease-linked variant as shown by multiple techniques, including a KI mouse model, cardiac electrophysiology, and cellular and molecular investigations. The KI mice bearing this variant displayed stress-induced arrhythmias, exhibiting some resemblance to the human p.Q1283H carrier's phenotype. Spontaneous SR Ca^{2+} release caused by RyR2 hyperphosphorylation is a contributing factor of the increased frequency of DADs and trigger activity. Mechanistically, the dissociation of PP2A from RyR2, characterized by a highly phosphorylated state of RyR2, is likely attributable to the reduced binding of AnkB to B56α. Finally, the administration of metoprolol or flecainide appears to be effective for managing p.Q1283H-induced arrhythmias.

Nearly all previously reported, likely deleterious *ANK2* variants are located in the SBD or RD domains.[4] In contrast, the p.Q1283H is the first variant identified in the ZU5^C region. The minor allele frequency, *in silico* analyses, and in vitro functional assays are commonly used to characterize the function and mechanistic rationale of *ANK2* variants. More important, the

introduction of a mutant AnkB construct into cardiomyocytes from AnkB$^{+/-}$ mice is unable to restore its abnormal functional activity, indirectly supporting a disease-associated variant.[1–3] Nevertheless, compared with AnkB$^{+/-}$ mice with a large genetic intervention, KI mice bearing a specific *ANK2* variant can be more valuable tools for directly characterizing its disease risk.[28] Although KI mice homozygous for *ANK2* p.L1622I produce cardiac electric phenotypes,[11] they cannot completely reproduce the human phenotype because heterozygous p.L1622I is more common in clinical settings. In contrast, we used heterozygous KI mice to mimic the heterozygous state of the human p.Q1283H carrier, and the mice displayed similarities to the arrhythmia phenotype of the patient.

Although similar phenotypes may result from different variants, the molecular mechanism underlying each variant can be distinct. *ANK2* variants may interfere with normal AnkB function by modulating intramolecular interactions.[29] For example, RD interacts with the amino-terminus of the membrane-binding domain to modulate its protein association with Ca^{2+} channels and transporters, and these associations can be impaired by *ANK2* variants in the RD.[4] In contrast, *ANK2* variants participate in modulating its interactions with its targeting proteins.[30] For example, the p.R1788W variant in the C-terminal domain directly abolishes AnkB binding to human DnaJ homologue 1.[31] The p.R990Q variant in ZU5^N leads to a severe arrhythmia phenotype by interfering with its binding to βII-spectrin.[32] However, our p.Q1283H variant located in the ZU5^C region did not affect its interaction with βII spectrin. In line with our findings, a number of synthetic *ANK2* variants in the ZU5^C region do not affect the βII-spectrin binding but still impair the function of AnkB.[33] It is important to note that nearly all reported *ANK2* variants result in a reduced abundance of AnkB, leading to altered intracellular Ca^{2+} dynamics linked with the abnormal expression and localization of Na$^+$/Ca^{2+} exchanger type 1, Na$^+$/K$^+$ ATPase α1/α2, and inositol 1,4,5-trisphosphate receptor.[4] The p.Q1283H variant did not alter the expression or subcellular distribution of AnkB. Therefore, beyond disturbed AnkB/βII spectrin binding or functional AnkB haploinsufficiency, previously unrecognized pathophysiological mechanisms that contribute to the processes of arrhythmias may exist.

In our study, patch-clamped KI myocytes showed an increased incidence of DAD-related trigger activity during ISO challenge. DADs are initiated by inward-mode Na$^+$/Ca^{2+} exchanger activation in response to spontaneous increases in the cytoplasmic Ca^{2+} concentration, which generates a transient depolarizing current.[34] If DADs reach the threshold for sarcolemmal Na$^+$ channels, an AP may be triggered and propagated through the myocardium, ultimately precipitating arrhythmias. It is thought that diastolic SR Ca^{2+} release via hyperactive

RyR2 is the primary molecular basis for Ca^{2+}-dependent DADs.[13] Indeed, KI cardiomyocytes demonstrated an arrhythmogenic increase in spontaneous Ca^{2+} waves and SR Ca^{2+} leak, particularly after ISO challenge. Ryanodine rescued these components of abnormal Ca^{2+} signaling, demonstrating that abnormally high RyR2 activity potentially underlies dysfunctional Ca^{2+} regulation. In parallel with the upregulation of an RyR2-mediated SR Ca^{2+} leak, the SR Ca^{2+} content was decreased in KI cardiomyocytes. An upregulated RyR2-mediated SR Ca^{2+} leak is an underlying cause of a reduced SR Ca^{2+} content,[35,36] resulting in proarrhythmic remodeling of Ca^{2+} homeostasis and arrhythmias.[37]

It is well known that the phosphorylation of RyR2 at Ser2814 plays a more important role in arrhythmogenic SR Ca^{2+} release than that of RyR2 at Ser2808.[16] In our KI model, the phosphorylation of RyR2 at Ser2814 was significantly increased under both basal and stress conditions. The inhibition of CaMKII by KN93 normalized this hyperphosphorylation and successfully antagonized the β-adrenergic effects and the triggering of ventricular arrhythmias.[17] Thus, the dysregulation of intracellular Ca^{2+} cycling because of RyR2 hyperphosphorylation potentially contributes to DAD-related trigger activity. Furthermore, the adaptive changes in intracellular Ca^{2+} homeostasis were in agreement with the dynamic changes in the phosphorylation of RyR2 at Ser2814. Under basal conditions, arrhythmias and arrhythmogenic SR Ca^{2+} release events did not occur despite the increased phosphorylation of RyR2 at Ser2814, suggesting that RyR2 Ser2814 alone is not sufficient to generate arrhythmias. After adding ISO to KI myocytes, β-adrenoceptor activation led to further abnormally enhanced phosphorylation of RyR2 at Ser2814 and functional disturbance. In fact, the p.Q1283H variant promoted the phosphorylation of RyR2 at Ser2814 at baseline and led to a highly arrhythmogenic state under conditions of increased sympathetic drive.

Experimental data suggest that alterations in local phosphatase activity toward specific substrates may be more harmful than alterations in the total phosphatase activity in cardiomyocytes.[19,37,38] Likewise, in our KI hearts, downregulated local PP2A holoenzyme populations may be an explanation for the RyR2 hyperphosphorylation. The additional targets of PP2A-Cav1.2 and PLN exhibited unchanged phosphorylation states, suggesting that PP2A-based RyR2 dephosphorylation is mutation specific in this KI model. Similar arrhythmic substrates in different murine models may result from distinct molecular mechanisms. In the AnkB$^{+/-}$ mouse model, RyR2 hyperphosphorylation associated with spontaneous SR Ca^{2+} release contributes to sympathetically mediated arrhythmias.[6,39,40] This RyR2 hyperphosphorylation in AnkB$^{+/-}$ hearts is CaMKII dependent because of increased junctional Ca^{2+},[39] whereas defects in the PP2A-based signaling pathway facilitate the phosphorylation of RyR2 in

our KI model. It appears that there is no need for CaMKII to be overactive because limited activity without CaMKII activation is sufficient to phosphorylate RyR2 in the absence of phosphatases.[9,41,42]

Several groups have investigated the specific sites of RyR2 dephosphorylation that are controlled by phosphatases, but their findings have been controversial. Little et al[8] demonstrated that the upregulation of PP2A activity decreased RyR2 phosphorylation at both Ser2814 and Ser2808. However, our findings demonstrated that changes in the local PP2A activity only dephosphorylated RyR2 at Ser2814. Consistently, Huke and Bers[43] demonstrated that PP1 preferentially controls RyR2 phosphorylation at Ser2808, whereas RyR2 Ser2814 is under the specific control of PP2A. Muscle-specific microRNAs mediating the suppression of PP2A activity in the RyR2 microdomain appear to regulate the phosphorylation of Ser2814.[9,23] It is important to note that the recognition of specific sites by the PP2A family may involve the additive effects of multiple distinct interactions, which could be a topic of cardiovascular research in follow-up studies.

AnkB is essential for targeting B56α,[10] which in turn tethers PP2A to the RyR2 complex.[9] B56α overexpression in vivo does not alter the expression of AnkB,[44] whereas primary cardiomyocytes from AnkB-deficient mice display an increased abundance and disorganized distribution of B56α.[8,10] In addition, AnkB localizes with inositol 1,4,5-trisphosphate receptor in a compartment distinct from RyR2,[45] suggesting that AnkB does not form a stable complex with RyR2 and thus does not directly modify RyR2 activity. We speculate that AnkB-mediated RyR2 hyperactivity is likely linked to the modulation of B56α. It remains a subject of debate whether the regulation of B56α mediates the activity of PP2A or RyR2.[16] Although the short-term expression of B56α in vitro does not alter PP2Ac expression,[46] the cardiac-specific overexpression of B56α in transgenic mice leads to a compensatory increase in PP2Ac expression and activity.[44] In contrast, the inhibition of B56α expression causes profound changes in PP2A activity, subsequently causing RyR2 dysfunction.[8,9] In our study, cardiac expression of mutant AnkB impaired the binding ability of the PP2A/B56α complex to RyR2 at specialized myocyte subdomains. We summarize that the AnkB-based abnormal spatial distribution of B56α leads to the dissociation of local PP2A from RyR2, subsequently resulting in RyR2 hyperphosphorylation.

The management of AnkB-based arrhythmias mainly depends on the defined clinical features of the patients. In our KI mice, metoprolol reduced the incidence of stress-induced ventricular arrhythmias. However, some patients with *ANK2* variants, such as R1788W,[2] S646F,[47] and W1535R,[48] are refractory to β-blocker therapy; therefore, more effective therapeutic options are required. In our KI mice, flecainide mitigated the risk of stress-induced ventricular arrhythmias. In isolated KI myocytes, flecainide had no effect on ISO-induced SCaTs, but it significantly inhibited triggered events, suggesting that the inhibitory effect of flecainide may not be because of its direct blocking of open-state RyR2.[49] As previously reported, this inhibitory action is likely because of the inhibition of subsarcolemmal Na^+ channels[25] or the modification of the Na^+/Ca^{2+} exchanger activity.[50] Finally, understanding the underlying molecular mechanisms of arrhythmias is helpful for developing possible precision therapies. AnkB may indirectly regulate the function of RyR2 by modulating the activity of PP2A, suggesting a novel therapeutic target for arrhythmias.

Several limitations should be considered in this study. First, because our experiments are confined to young adult animals, future studies should focus on older animals to determine whether they exhibit more severe phenotypes. Second, although mouse models provide insight into the mechanisms of human disease, inherent differences between human and mouse physiology must ultimately be considered when interpreting our findings. Thus, although our findings support the mechanisms underlying this human condition, we recognize that there may be pathophysiological differences. Finally, we mainly focused on the susceptibility of KI mice to arrhythmias under acute stress. However, whether an increased sympathetic input to the heart tunes Ca^{2+} homeostasis in chronic disease is still unknown.

In conclusion, we first identified a disease-associated p.Q1283H variant in *ANK2*-ZU5^C that is responsible for arrhythmias, which may be treated with metoprolol or flecainide. We found that the dysregulation of intracellular Ca^{2+} cycling because of RyR2 hyperphosphorylation potentially contributes to DAD-related trigger activity. Additionally, the combination of enhanced adrenergic activity and the loss of PP2A activity from RyR2, which is likely associated with reduced AnkB/B56α binding, provides the underlying molecular mechanisms of the diastolic SR Ca^{2+} release. Our findings provide new insights into the functional role of AnkB, as well as the potential pathogenesis of and the therapeutic options for AnkB-based arrhythmias.

ARTICLE INFORMATION

Correspondence

Kui Hong, MD, PhD, Department of Cardiovascular Medicine and Jiangxi Key Laboratory of Molecular Medicine, The Second Affiliated Hospital of Nanchang University, No.1, Minde Road, Nanchang of Jiangxi, 330006; or Peter J. Mohler, PhD, Dorothy M. Davis Heart and Lung Research Institute, 473 W 12th Avenue, DHLRI 110G, Columbus, OH 43210. Email hongkui88@163.com or peter.mohler@osumc.edu

REFERENCES

1. Mohler PJ, Le Scouarnec S, Denjoy I, Lowe JS, Guicheney P, Caron L, Driskell IM, Schott JJ, Norris K, Leenhardt A, Kim RB, Escande D, Roden DM. Defining the cellular phenotype of "ankyrin-B syndrome" variants: human ANK2 variants associated with clinical phenotypes display a spectrum of activities in cardiomyocytes. *Circulation*. 2007;115:432–441. doi: 10.1161/CIRCULATIONAHA.106.656512

2. Mohler PJ, Splawski I, Napolitano C, Bottelli G, Sharpe L, Timothy K, Priori SG, Keating MT, Bennett V. A cardiac arrhythmia syndrome caused by loss of ankyrin-B function. *Proc Natl Acad Sci U S A*. 2004;101:9137–9142. doi: 10.1073/pnas.0402546101

3. Mohler PJ, Schott JJ, Gramolini AO, Dilly KW, Guatimosim S, DuBell WH, Song LS, Haurogne K, Kyndt F, Ali ME, Rogers TB, Lederer WJ, Escande D, Le Marec H, Bennett V. Ankyrin-B mutation causes type 4 long-QT cardiac arrhythmia and sudden cardiac death. *Nature*. 2003;421:634–639. doi: 10.1038/nature01335

4. Koenig SN, Mohler PJ. The evolving role of ankyrin-B in cardiovascular disease. *Heart Rhythm*. 2017;14:1884–1889. doi: 10.1016/j.hrthm.2017.07.032

5. Wang C, Yu C, Ye F, Wei Z, Zhang M. Structure of the ZU5-ZU5-UPA-DD tandem of ankyrin-B reveals interaction surfaces necessary for ankyrin function. *Proc Natl Acad Sci U S A*. 2012;109:4822–4827. doi: 10.1073/pnas.1200613109

6. DeGrande S, Nixon D, Koval O, Curran JW, Wright P, Wang Q, Kashef F, Chiang D, Li N, Wehrens XHT, Anderson ME, Hund TJ, Mohler PJ. CaMKII inhibition rescues proarrhythmic phenotypes in the model of human ankyrin-B syndrome. *Heart Rhythm*. 2012;9:2034–2041. doi: 10.1016/j.hrthm.2012.08.026

7. Lubbers ER, Mohler PJ. Roles and regulation of protein phosphatase 2A (PP2A) in the heart. *J Mol Cell Cardiol*. 2016;101:127–133. doi: 10.1016/j.yjmcc.2016.11.003

8. Little SC, Curran J, Makara MA, Kline CF, Ho HT, Xu Z, Wu X, Polina I, Musa H, Meadows AM, Carnes CA, Biesiadecki BJ, Davis JP, Weisleder N, Györke S, Wehrens XH, Hund TJ, Mohler PJ. Protein phosphatase 2A regulatory subunit B56α limits phosphatase activity in the heart. *Sci Signal*. 2015;8:ra72. doi: 10.1126/scisignal.aaa5876

9. Terentyev D, Belevych AE, Terentyeva R, Martin MM, Malana GE, Kuhn DE, Abdellatif M, Feldman DS, Elton TS, Györke S. miR-1 overexpression enhances Ca(2+) release and promotes cardiac arrhythmogenesis by targeting PP2A regulatory subunit B56alpha and causing CaMKII-dependent hyperphosphorylation of RyR2. *Circ Res*. 2009;104:514–521. doi: 10.1161/CIRCRESAHA.108.181651

10. Bhasin N, Cunha SR, Mudannayake M, Gigena MS, Rogers TB, Mohler PJ. Molecular basis for PP2A regulatory subunit B56alpha targeting in cardiomyocytes. *Am J Physiol Heart Circ Physiol*. 2007;293:H109–H119. doi: 10.1152/ajpheart.00059.2007

11. Musa H, Murphy NP, Curran J, Higgins JD, Webb TR, Makara MA, Wright P, Lancione PJ, Lubbers ER, Healy JA, Smith SA, Bennett V, Hund TJ, Kline CF, Mohler PJ. Common human ANK2 variant confers in vivo arrhythmia phenotypes. *Heart Rhythm*. 2016;13:1932–1940. doi: 10.1016/j.hrthm.2016.06.012

12. Curtis MJ, Walker MJ. Quantification of arrhythmias using scoring systems: an examination of seven scores in an *in vivo* model of regional myocardial ischaemia. *Cardiovasc Res*. 1988;22:656–665.

13. Landstrom AP, Dobrev D, Wehrens XHT. Calcium signaling and cardiac arrhythmias. *Circ Res*. 2017;120:1969–1993. doi: 10.1161/CIRCRESAHA.117.310083

14. Cheng H, Lederer MR, Lederer WJ, Cannell MB. Calcium sparks and [Ca2+]i waves in cardiac myocytes. *Am J Physiol*. 1996;270(1 Pt 1):C148–C159. doi: 10.1152/ajpcell.1996.270.1.C148

15. Nelson BR, Makarewich CA, Anderson DM, Winders BR, Troupes CD, Wu F, Reese AL, McAnally JR, Chen X, Kavalali ET, Cannon SC, Houser SR, Bassel-Duby R, Olson EN. A peptide encoded by a transcript annotated as long noncoding RNA enhances SERCA activity in muscle. *Science*. 2016;351:271–275. doi: 10.1126/science.aad4076

16. Dobrev D, Wehrens XHT. Role of RyR2 phosphorylation in heart failure and arrhythmias: controversies around ryanodine receptor phosphorylation in cardiac disease. *Circ Res*. 2014;114:1311–1319. doi: 10.1161/CIRCRESAHA.114.300568

17. Tzimas C, Terrovitis J, Lehnart SE, Kranias EG, Sanoudou D. Calcium/calmodulin-dependent protein kinase II (CaMKII) inhibition ameliorates arrhythmias elicited by junctin ablation under stress conditions. *Heart Rhythm*. 2015;12:1599–1610. doi: org/10.1016/j.hrthm.2015.03.043

18. Curran J, Hinton MJ, Rios E, Bers DM, Shannon TR. Beta-adrenergic enhancement of sarcoplasmic reticulum calcium leak in cardiac myocytes is mediated by calcium/calmodulin-dependent protein kinase. *Circ Res*. 2007;100:391–398. doi: 10.1161/01.RES.0000258172.74570.e6

19. Marx SO, Reiken S, Hisamatsu Y, Jayaraman T, Burkhoff D, Rosemblit N, Marks AR. PKA phosphorylation dissociates FKBP12.6 from the calcium release channel (ryanodine receptor): defective regulation in failing hearts. *Cell*. 2000;101:365–376.

20. Chung H, Nairn AC, Murata K, Brautigan DL. Mutation of Tyr307 and Leu309 in the protein phosphatase 2A catalytic subunit favors association with the alpha 4 subunit which promotes dephosphorylation of elongation factor-2. *Biochemistry*. 1999;38:10371–10376. doi: 10.1021/bi990902g

21. Lei M, Wang X, Ke Y, Solaro RJ. Regulation of Ca2+ transient by PP2A in normal and failing heart. *Front Physiol*. 2015;6:13. doi: 10.3389/fphys.2015.00013

22. Dodge-Kafka KL, Bauman A, Mayer N, Henson E, Heredia L, Ahn J, McAvoy T, Nairn AC, Kapiloff MS. cAMP-stimulated protein phosphatase 2A activity associated with muscle A kinase-anchoring protein (mAKAP) signaling complexes inhibits the phosphorylation and activity of the cAMP-specific phosphodiesterase PDE4D3. *J Biol Chem*. 2010;285:11078–11086. doi: 10.1074/jbc.M109.034868

23. Belevych AE, Sansom SE, Terentyeva R, Ho HT, Nishijima Y, Martin MM, Jindal HK, Rochira JA, Kunitomo Y, Abdellatif M, Carnes CA, Elton TS, Gyorke S, Terentyev D. MicroRNA-1 and -133 increase arrhythmogenesis in heart failure by dissociating phosphatase activity from RyR2 complex. *Plos One*. 2011;6:e28324. doi: 10.1371/journal.pone.0028324

24. Marx SO, Reiken S, Hisamatsu Y, Gaburjakova M, Gaburjakova J, Yang YM, Rosemblit N, Marks AR. Phosphorylation-dependent regulation of ryanodine receptors: a novel role for leucine/isoleucine zippers. *J Cell Biol*. 2001;153:699–708. doi: 10.1083/jcb.153.4.699

25. Liu N, Denegri M, Ruan Y, Avelino-Cruz JE, Perissi A, Negri S, Napolitano C, Coetzee WA, Boyden PA, Priori SG. Short communication: flecainide exerts an antiarrhythmic effect in a mouse model of catecholaminergic polymorphic ventricular tachycardia by increasing the threshold for triggered activity. *Circ Res*. 2011;109:291–295. doi: 10.1161/CIRCRESAHA.111.247338

26. Kannankeril PJ, Moore JP, Cerrone M, Priori SG, Kertesz NJ, Ro PS, Batra AS, Kaufman ES, Fairbrother DL, Saarel EV, Etheridge SP, Kanter RJ, Carboni MP, Dzurik MV, Fountain D, Chen H, Ely EW, Roden DM, Knollmann BC. Efficacy of flecainide in the treatment of catecholaminergic polymorphic ventricular tachycardia: a randomized clinical trial. *JAMA Cardiol*. 2017;2:759–766. doi: 10.1001/jamacardio.2017.1320

27. Watanabe H, Chopra N, Laver D, Hwang HS, Davies SS, Roach DE, Duff HJ, Roden DM, Wilde AAM, Knollmann BC. Flecainide prevents catechol-

aminergic polymorphic ventricular tachycardia in mice and humans. *Nat Med*. 2009;15:380–383. doi: 10.1038/nm.1942

28. Fu Y, Xiao S, Hong T, Shaw RM. Cytoskeleton regulation of ion channels. *Circulation*. 2015;131:689–691. doi: 10.1161/CIRCULATIONAHA.115.015216

29. Abdi KM, Mohler PJ, Davis JQ, Bennett V. Isoform specificity of ankyrin-B: a site in the divergent C-terminal domain is required for intramolecular association. *J Biol Chem*. 2006;281:5741–5749. doi: 10.1074/jbc.M506697200

30. Cunha SR, Mohler PJ. Obscurin targets ankyrin-B and protein phosphatase 2A to the cardiac M-line. *J Biol Chem*. 2008;283:31968–31980. doi: 10.1074/jbc.M806050200

31. Mohler PJ, Hoffman JA, Davis JQ, Abdi KM, Kim CR, Jones SK, Davis LH, Roberts KF, Bennett V. Isoform specificity among ankyrins: an amphipathic alpha-helix in the divergent regulatory domain of ankyrin-b interacts with the molecular co-chaperone Hdj1/Hsp40. *J Biol Chem*. 2004;279:25798–25804. doi: 10.1074/jbc.M401296200

32. Smith SA, Sturm AC, Curran J, Kline CF, Little SC, Bonilla IM, Long VP, Makara M, Polina I, Hughes LD, Webb TR, Wei Z, Wright P, Voigt N, Bhakta D, Spoonamore KG, Zhang C, Weiss R, Binkley PF, Janssen PM, Kilic A, Higgins RS, Sun M, Ma J, Dobrev D, Zhang M, Carnes CA, Vatta M, Rasband MN, Hund TJ, Mohler PJ. Dysfunction in the βII spectrin-dependent cytoskeleton underlies human arrhythmia. *Circulation*. 2015;131:695–708. doi: 10.1161/CIRCULATIONAHA.114.013708

33. Kizhatil K, Yoon W, Mohler PJ, Davis LH, Hoffman JA, Bennett V. Ankyrin-G and beta2-spectrin collaborate in biogenesis of lateral membrane of human bronchial epithelial cells. *J Biol Chem*. 2007;282:2029–2037. doi: 10.1074/jbc.M608921200

34. Pogwizd SM, Schlotthauer K, Li L, Yuan W, Bers DM. Arrhythmogenesis and contractile dysfunction in heart failure: roles of sodium-calcium exchange, inward rectifier potassium current, and residual beta-adrenergic responsiveness. *Circ Res*. 2001;88:1159–1167. doi: org/10.1161/hh1101.091193

35. Tzimas C, Johnson DM, Santiago DJ, Vafiadaki E, Arvanitis DA, Davos CH, Varela A, Athanasiadis NC, Dimitriou C, Katsimpoulas M, Sonntag S, Kryzhanovska M, Shmerling D, Lehnart SE, Sipido KR, Kranias EG, Sanoudou D. Impaired calcium homeostasis is associated with sudden cardiac death and arrhythmias in a genetic equivalent mouse model of the human HRC-Ser96Ala variant. *Cardiovasc Res*. 2017;113:1403–1417. doi: 10.1093/cvr/cvx113

36. Fernandez-Velasco M, Rueda A, Rizzi N, Benitah JP, Colombi B, Napolitano C, Priori SG, Richard S, Gomez AM. Increased Ca2+ sensitivity of the ryanodine receptor mutant RyR2R4496C underlies catecholaminergic polymorphic ventricular tachycardia. *Circ Res*. 2009;104:201–209. doi: 10.1161/CIRCRESAHA.108.177493

37. Ai X, Curran JW, Shannon TR, Bers DM, Pogwizd SM. Ca2+/calmodulin-dependent protein kinase modulates cardiac ryanodine receptor phosphorylation and sarcoplasmic reticulum Ca2+ leak in heart failure. *Circ Res*. 2005;97:1314–1322. doi: 10.1161/01.RES.0000194329.41863.89

38. Reiken S, Gaburjakova M, Gaburjakova J, He KK, Prieto A, Becker E, Yi GG, Wang J, Burkhoff D, Marks AR. Beta-adrenergic receptor blockers restore cardiac calcium release channel (ryanodine receptor) structure and function in heart failure. *Circulation*. 2001;104:2843–2848. doi: org/10.1161/hc4701.099578

39. Popescu I, Galice S, Mohler PJ, Despa S. Elevated local [Ca2+] and CaMKII promote spontaneous Ca2+ release in ankyrin-B-deficient hearts. *Cardiovasc Res*. 2016;111:287–294. doi: 10.1093/cvr/cvw093

40. Camors E, Mohler PJ, Bers DM, Despa S. Ankyrin-B reduction enhances Ca spark-mediated SR Ca release promoting cardiac myocyte arrhythmic activity. *J Mol Cell Cardiol*. 2012;52:1240–1248. doi: 10.1016/j.yjmcc.2012.02.010

41. Terentyev D, Rees CM, Li W, Cooper LL, Jindal HK, Peng X, Lu Y, Terentyeva R, Odening KE, Daley J, Bist K, Choi BR, Karma A, Koren G. Hyperphosphorylation of RyRs underlies triggered activity in transgenic rabbit model of LQT2 syndrome. *Circ Res*. 2014;115:919–928. doi: 10.1161/CIRCRESAHA.115.305146

42. DeGrande ST, Little SC, Nixon DJ, Wright P, Snyder J, Dun W, Murphy N, Kilic A, Higgins R, Binkley PF, Boyden PA, Carnes CA, Anderson ME, Hund TJ, Mohler PJ. Molecular mechanisms underlying cardiac protein phosphatase 2A regulation in heart. *J Biol Chem*. 2013;288:1032–1046. doi: 10.1074/jbc.M112.426957

43. Huke S, Bers DM. Ryanodine receptor phosphorylation at Serine 2030, 2808 and 2814 in rat cardiomyocytes. *Biochem Biophys Res Commun*. 2008;376:80–85. doi: 10.1016/j.bbrc.2008.08.084

44. Kirchhefer U, Brekle C, Eskandar J, Isensee G, Kucerova D, Muller FU, Pinet F, Schulte JS, Seidl MD, Boknik P. Cardiac function is regulated by B56alpha-mediated targeting of protein phosphatase 2A (PP2A) to contractile relevant substrates. *J Biol Chem*. 2014;289:33862–33873. doi: 10.1074/jbc.M114.598938

45. Tuvia S, Buhusi M, Davis L, Reedy M, Bennett V. Ankyrin-B is required for intracellular sorting of structurally diverse Ca2+ homeostasis proteins. *J Cell Biol*. 1999;147:995–1008. doi: 10.1083/jcb.147.5.995

46. Gigena MS, Ito A, Nojima H, Rogers TB. A B56 regulatory subunit of protein phosphatase 2A localizes to nuclear speckles in cardiomyocytes. *Am J Physiol Heart Circ Physiol*. 2005;289:H285–H294. doi: 10.1152/ajpheart.01291.2004

47. Swayne LA, Murphy NP, Asuri S, Chen L, Xu X, McIntosh S, Wang C, Lancione PJ, Roberts JD, Kerr C, Sanatani S, Sherwin E, Kline CF, Zhang M, Mohler PJ, Arbour LT. Novel variant in the ANK2 membrane-binding domain is associated with ankyrin-B syndrome and structural heart disease in a first nations population with a high rate of long QT syndrome. *Circ Cardiovasc Genet*. 2017;10:e1537. doi: 10.1161/CIRCGENETICS.116.001537

48. Ichikawa M, Aiba T, Ohno S, Shigemizu D, Ozawa J, Sonoda K, Fukuyama M, Itoh H, Miyamoto Y, Tsunoda T, Makiyama T, Tanaka T, Shimizu W, Horie M. Phenotypic variability of ANK2 mutations in patients with inherited primary arrhythmia syndromes. *Circ J*. 2016;80:2435–2442. doi: 10.1253/circj.CJ-16–0486

49. Bannister ML, Thomas NL, Sikkel MB, Mukherjee S, Maxwell C, MacLeod KT, George CH, Williams AJ. The mechanism of flecainide action in CPVT does not involve a direct effect on RyR2. *Circ Res*. 2015;116:1324–1335. doi: 10.1161/CIRCRESAHA.116.305347

50. Sikkel MB, Collins TP, Rowlands C, Shah M, O'Gara P, Williams AJ, Harding SE, Lyon AR, MacLeod KT. Flecainide reduces Ca(2+) spark and wave frequency via inhibition of the sarcolemmal sodium current. *Cardiovasc Res*. 2013;98:286–296. doi: 10.1093/cvr/cvt012.